JOURNAL OF AGRICULTURAL AND FOOD CHEMISTRY

Article

Cite This: J. Agric. Food Chem. 2018, 66, 3101−3109

pubs.acs.org/JAFC

Preparation, Characterization, and *In Vitro* Testing of Nanoclay Antimicrobial Activities and Elicitor Capacity

Danila Merino,*[,†] Andrea Y. Mansilla,[‡] Claudia A. Casalongué,[‡] and Vera A. Alvarez[†]

[†]Grupo de Materiales Compuestos Termoplásticos (CoMP), Instituto de Investigaciones en Ciencia y Tecnología de Materiales (INTEMA), Universidad Nacional de Mar del Plata−Concejo Nacional de Investigaciones Científicas y Técnicas (CONICET), Colon 10890, 7600 Mar del Plata, Argentina

[‡]Instituto de Investigaciones Biológicas, UE CONICET−UNMdP, Facultad de Ciencias Exactas y Naturales, Universidad Nacional de Mar del Plata, Deán Funes 3250, 7600 Mar del Plata, Argentina

Supporting Information

ABSTRACT: Clay-based nanocomposites (nanoclays) are interesting systems to hold a wide type of active substances with a wide field of industrial applications. Bentonite−chitosan nanoclay was obtained via cationic exchange of natural bentonite (Bent) with an aqueous solution of chitosan (CS). Their physicochemical and morphological properties were discussed under the light of Fourier transform infrared spectroscopy, X-ray diffraction, thermogravimetric analysis, and scanning electron microscopy. Bent−CS characterization indicated that CS was intercalated in 10% (w/w). This polycationic polymer was oriented mostly in a monolayer arrangement, interacting by electrostatic forces between Bent sheets. The antimicrobial action of Bent−CS nanoclay was assayed onto phytopathogens, the bacterium model *Pseudomonas syringe* pv. *tomato* DC3000 (*Psy*) and the necrotrophic fungus *Fusarium solani* f. sp. *eumartii* (*F. eumartii*). In addition to demonstrating cell death on both microorganisms, Bent−CS exerted elicitor property on tomato plantlets. The biological actions of this natural nanomaterial might make it proper to be used in crops.

KEYWORDS: *bentonite, chitosan, nanocomposite, antibacterial, antifungal, elicitor*

1. INTRODUCTION

Currently, agriculture is going through a period of significant challenges marked by climate change, urbanization, and environmental issues, such as the accumulation of pesticides and fertilizers. In parallel, the great growth of the world population that is expected to exceed 9 billion by 2050[1] makes the need to carry out new innovative developments committed to the care of the environment and sustainable solutions evident.[2]

Nanoclays are clay minerals that have at least one of their dimensions in the nanometer range. They are included within a wide variety of clay minerals and refer mainly to the phyllosilicates. Phyllosilicates are stratified aluminosilicates. They consist of layers of aluminum and silicon oxides stacked on top of each other.[3,4] Among them, montmorillonite (MMT), whose structure is introduced in Scheme 1, is notable for its wide abundance and large aspect ratio: it has an interlamellar spacing of approximately 1 nm, and its sheets a length between 200 and 600 nm.[3]

Bentonite (Bent) is a type of clay composed mainly of MMT. It stands out for its high cation-exchange capacity (CEC), large surface area, porosity, and small particle size.[4] A not widespread application of Bent is its use as an amendment in sandy soils. This type of soil has a low clay content and, therefore, a low CEC.[5] Soils with these characteristics do not have the capacity to retain and supply the necessary nutrients for the plants, which consequently produces low yields. Current agricultural practices contemplate for these cases the addition of large quantities of fertilizers, but given that the soil has low CEC, these are quickly lost by leaching, leaving in evidence the poor economic and environmental sustainability of the current agricultural system.[6]

Scheme 1. Chemical Structure of MMT

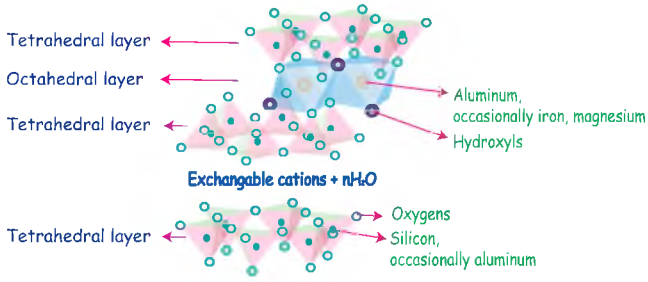

In this context, countries, such as China,[7] Thailand,[8] Australia,[6] Poland,[5] and Uganda,[9] have considered adding Bent to their light textured sandy soils to increase their CEC.[8] Published papers report significant increments in crop yields over consecutive years, increments in water retention,[7,8] improved nutrient retention and availability, and greater fertilizer use efficiency.[6,9] Additionally, the Food and Agriculture Organization of the United Nations (FAO) recognizes Bent as a permitted substance for the production of organic foods in the categories "substances for use in soil fertilizing and conditioning", "substances for plant pest and disease control", and "processing aids which may be used for the preparation of products of agricultural origin".[10]

Received: January 3, 2018
Revised: March 1, 2018
Accepted: March 6, 2018
Published: March 6, 2018

DOI: 10.1021/acs.jafc.8b00049
J. Agric. Food Chem. 2018, 66, 3101−3109

As mentioned above, Bent has among other benefits, a large CEC and, consequently, the possibility of lodging organic cations between its sheets.[11] Chitosan (CS) is a linear chain cationic polymer derived from chitin, the second most abundant polymer in nature.[12,13] It has been shown that CS causes cell death in a large variety of pathogenic fungi and inhibits the growth of pathogenic bacteria. It is even capable of inactivating the replication of viruses and viroids.[14] It has been well-demonstrated that CS induces numerous biological responses in plants and improves defense responses to biotic and abiotic stresses.[15,16] When a plant is infected by a pathogen, it responds by means of the induction of an innate defense mechanism. The molecules that possess the ability to activate these defense mechanisms of plants are called "elicitors".[14] The knowledge about the biochemical and molecular mechanisms of plant defense responses has allowed artificially inducing defense responses using a chemical inductor or natural elicitors.[17] In this sense, the use of CS is becoming very important because it is an environmentally friendly polymer for protecting crops.[15] CS represents an alternative to the use of toxic pesticides for the treatment of several phytopathogens, including bacteria, fungi, virus, and nematodes.[14,18−20] Thus, CS can be a promising candidate to safely control plant diseases. However, it is important to mention that direct utilization of CS in crop protection has several disadvantages, such as its solubility in mild acid media, its volatilization, leaching, and the need of being applied repetitively in time to avoid using high doses.

In this work, tomato (*Solanum lycopersicum*), which is a cultivated horticultural plant species worldwide,[21] was used as a study model. *Pseudomonas syringae* pv. *tomato* (*Psy*) is a Gram-negative bacterium and the causal agent of the bacterial spot in tomato, which is a disease for which effective controls are still needed. The incidence of this disease causes severe loss of yield and fruit quality.[22] Additionally, the wilt caused by the pathogenic fungus *Fusarium solani* f. sp. *eumartii* (*F. eumartii*) is a negative cause in tomato production and yield.[23]

The aim of this work was to obtain and characterize a CS-functionalized nanoclay with combined actions as an antimicrobial and plant elicitor compound. For that, Bent and Bent−CS were analyzed by Fourier transform infrared spectroscopy (FTIR), X-ray diffraction (XRD), and thermogravimetric analysis (TGA). In addition, the functions of Bent−CS as an antimicrobial agent against *Psy* and *F. eumartii* and plant elicitor are discussed.

MATERIALS AND METHODS

Materials. Bent used was obtained from Minarmco S.A. (Neuquén, Argentina) and was used as received. Its CEC was 105 mequiv/100 g of clay, determined by the methylene blue method. It was mainly composed of MMT with quartz and feldspar as principal impurities and presented traces of gypsum and sepiolite.[24] CS used for the preparation of the nanoclay was obtained from Drogueria Sapporiti (Buenos Aires, Argentina). Its degree of deacetylation was greater than 90%, and its molar mass was 531 kDa. The acetic acid (HAc) used in the preparation of its solutions was obtained from Biopack (Buenos Aires, Argentina).

Biological Material and Growth. The experiments with plants were performed using tomato seeds (*S. lycopersicum*) of cv. Platense. Seedlings were grown on Murashige and Skoog (MS) medium[25] containing 0.8% (w/v) agar. After that, tomato plants were grown at 25 °C, with the light intensity of 120 μmol of photons m^{-2} s^{-1} and 16/8 h photoperiod. *Pys* was maintained on King's B (KB) agar medium[26] containing suitable antibiotics, 50 μg mL^{-1} rifampicin and 50 μg mL^{-1} kanamycin, according to Mansilla et al.[22] Single colonies grown at 30 °C for 48 h were isolated from agar plates, transferred to KB broth, and grown overnight at 30 °C with shaking. *F. eumartii* was obtained from Estación Experimental Agropecuaria (EEA), Instituto Nacional de Tecnología Agropecuaria (INTA), Balcarce, Argentina. Spores were harvested from 8-day-old cultures grown on solid potato dextrose agar (PDA) medium at 25 °C by adding 1 mL of sterile water to the plates and scraping the surface, Conidia were counted using a hemocytometer, diluted to the appropriate concentration and used for the assay.

Nanoclay Preparation. To obtain Bent−CS nanoclays, 1% (w/v) CS solution was prepared in 1% (v/v) HAc solution. After 1 h of stirring at room temperature, the CS solution (pH 3.6) was brought to pH 5.0 with 1 M NaOH and then poured onto a 1% (w/v) Bent dispersion in distilled water. Then, the mixture was stirred at 400 rpm and 60 °C. The nanoclays obtained were centrifuged, washed 3 times with distilled water, and lyophilized. To perform an optimization of the synthesis method, the initial CS/Bent ratio and the reaction time were studied. For the study of the CS/Bent ratio, the following concentrations were used: 0.025, 0.25, 0.50, and 0.75 g of CS/g of Bent and stirring was maintained for 2 h. To study the effect of the reaction time, different syntheses were carried out at a fixed CS/Bent ratio (0.25 g of CS/g of Bent) and by keeping stirring for 30, 60, and 120 min. Results showed that the maximum CS amount incorporated by Bent was about 10% (w/w); therefore, the 0.10 g of CS/g of Bent ratio and 30 min of reaction time were chosen as the optimal conditions to obtain Bent−CS nanoclay. This nanoclay will be referred to hereinafter as Bent−CS. The curves of the CS content retained by Bent as a function of the initial CS/Bent ratio and the reaction time are included in the Supporting Information.

Nanoclay Characterization Techniques. FTIR spectra, measured by attenuated total reflectance (ATR), were acquired with a Nicolet 6700 Thermo Scientific instrument, over the range of 400−4000 cm^{-1} from 32 co-added scans at 4 cm^{-1} resolution. Powder samples of Bent and Bent−CS were analyzed by XRD using an X'Pert Pro diffractometer, operating at 40 kV and 40 mA, with Cu Kα radiation (λ = 1.54 Å), at a scanning speed of 1°/min and step size of 0.02°. The basal reflections (d_{001} values) were calculated from the 2θ values using Bragg's equation (eq 1).

$$n\lambda = 2d \sin\theta \tag{1}$$

The shape, size, and arrangement of Bent and Bent−CS sheets were investigated by transmission electron microscopy (TEM). For that, a Jeol JEM 2100 transmission electron microscope was used at an operating voltage of 200 kV. The sample was well-dispersed in butanol. Then, a drop of it was placed on a holey carbon copper grid for TEM image obtention. Micrographs were obtained at 150000× magnification, and the "Image Pro Plus" software was used to perform the measurements.

TGA was performed with a TG HI-Res thermal analyzer (TA Instruments) at a heating rate of 10 °C/min from room temperature to 900 °C in air flow. The mass of all specimens was in the range of 20−30 mg. Organic mass contents were determined using eqs 2 and 3

$$M_{r,\text{Bent−CS}} = X_{\text{Bent}} M_{r,\text{Bent}} + X_{\text{CS}} M_{r,\text{CS}} \tag{2}$$

$$X_{\text{Bent}} + X_{\text{CS}} = 1 \tag{3}$$

where $M_{r,\text{Bent−CS}}$ is the residual mass of Bent−CS at 895 °C, X_{Bent} is the weight fraction of Bent in the nanoclay, $M_{r,\text{Bent}}$ is the residual mass of Bent at 895 °C, X_{CS} is the weight fraction of CS in the nanoclay, and $M_{r,\text{CS}}$ is the residual mass of pure CS at 895 °C. Bent and Bent−CS were also analyzed by scanning electron microscopy (SEM) to study their morphology. The microscope used was a FESEM Supra55, Zeiss (Germany), with an acceleration voltage of 3 kV. To ensure electrical conduction, samples were previously coated with gold by sputter with a 3 kV Ar^+ ion beam for 35 s.

Antimicrobial Assay. Cell viability was determined by propidium iodide (PI) exclusion.[27] PI is a fluorescent dye that cannot cross the membrane of live cells, making it useful to differentiate between living and dead cells. Briefly, the membrane of living cells forms a selectively permeable barrier between the content of the intracellular and extracellular media. Dead cells lose this property and, therefore, incorporate dye, which intercalates between the bases of DNA and

DOI: 10.1021/acs.jafc.8b00049
J. Agric. Food Chem. 2018, 66, 3101−3109

RNA.[28] For *Psy* cell death analysis, aliquots of overnight starter cultures of *Psy* were used to inoculate fresh KB liquid medium incubated with 10 mg/mL of Bent, 10 mg/mL of Bent−CS, and 1 mg/mL of CS or water at 30 °C overnight. For *F. eumartii*, spore suspension (1×10^7 spores mL^{-1}) was incubated with 10 mg/mL of Bent, 10 mg/mL of Bent−CS, and 1 mg/mL of CS (positive control) or water (negative control) for 4 h and 100% relative humidity at 25 °C in the dark. Then, PI was added in each well to a final concentration of 120 μM and then kept at room temperature for approximately 20 min in the dark. A total of 5 μL of the stained cell suspensions were deposited onto glass slides and covered with coverslips. Cells were photographed under a Nikon Eclipse E200 microscope equipped with an epifluorescence unit and a G-2E/C filter set containing an excitation filter at 540/25 nm, a suppressor filter at 630/60 nm, and a dichroic mirror at 565 nm. All treatments were performed in duplicate with an independent biological sample.

***In Planta* Assay.** The elicitor capacity of the nanoclays Bent and Bent−CS was determined through *in planta* bioassays. Sterile tomato seeds were placed in Petri dishes with MS agar under laminar flow. They were germinated at 25 °C with a photoperiod of 16 h of light (120 μmol of photons m^{-2} s^{-1}) and 8 h of darkness and controlled humidity. Tomato seedlings (10-day-old) were placed on MS agar plates, treated for 24 h with different concentrations of Bent or Bent−CS, and supplemented at the same concentration with a hand-held spray. The biological samples from each treatment were analyzed in three independent western blot assays.

Protein Extraction and Western Blot. Total soluble proteins were extracted with 1.5 volumes of protein extraction buffer (Agrisera, AS08 300). Denaturing electrophoresis in 12% sodium dodecyl sulfate polyacrylamide gel electrophoresis (SDS−PAGE) was performed according to Laemmli[29] using the Mini-PROTEAN II vertical gel system (BioRad, Hercules, CA, U.S.A.). The proteins previously separated by SDS−PAGE were transferred to nitrocellulose membranes (BioRad, Hercules, CA, U.S.A.). Immunodetection was performed using the polyclonal anti-glucanase antibody (Agrisera). The membranes were incubated with the secondary antibody conjugated to the enzyme alkaline phosphatase (Sigma-Aldrich, St. Louis, MO, U.S.A.). Reactions were developed with tetrazolium blue/5-bromo-4-Chloro-3-indolyl phosphate as substrates according to the instructions of the supplier (Sigma-Aldrich, St. Louis, MO, U.S.A.).

RESULTS AND DISCUSSION

Evidence about the formation of Bent−CS nanoclay was observed by FTIR, XRD, and TGA. These characterization techniques provide valuable information about CS and Bent chemical interactions, the molecular chain orientation of CS with respect to Bent sheets, and the amount of CS present in the final nanocomposite.

The presence of CS in the clay was confirmed by FTIR. Figure 1 shows the infrared absorption spectra of Bent and Bent−CS nanoclays.

The main absorption bands of Bent have appeared at 986 cm^{-1}, which corresponds with the stretching vibration frequency of Si−O, 1635 cm^{-1}, which is associated with the bending frequency of water molecules absorbed on the clay surface, 3400 cm^{-1}, corresponding to the stretching vibration frequency of O−H water molecules adsorbed on Bent, and a band centered at 3621 cm^{-1}, related to the stretching vibrations of structural O−H groups.[11,30,31]

When the Bent and Bent−CS infrared spectra were compared, some changes in specific band absorption intensities were observed. The broad band at 3500−3200 cm^{-1} related to the hydroxyl stretching bands has increased in the nanoclay, suggesting an increment in hydrogen bonding as a result of new interactions between the lattice hydroxyls of Bent and organic groups of CS. In addition, a reduction in Si−O band intensity is attributed to the weakening of Si−O bonds as a result of the formation of hydrogen bonds with CS.[32] Moreover, new

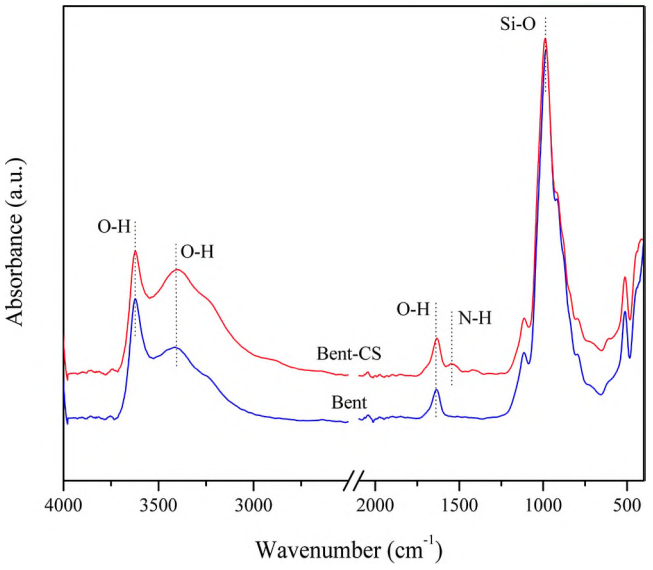

Figure 1. FTIR spectra of Bent and Bent−CS nanoclays. Changes in absorption band intensities and positions suggested a strong interaction between CS and Bent.

bands related to the absorption of CS molecules appeared in the spectra of Bent−CS. Bands centered at 2885 and 2946 cm^{-1} correspond to symmetric and antisymmetric stretching vibration frequencies of C−H at CH_3 groups present in the *N*-acetyl groups.[11,33] Pure CS spectra present bands centered at 1589 and 1645 cm^{-1}. The first band is due to the bending vibration of $-NH_2$.[33,34] The position of that band is usually between 1595 and 1550 cm^{-1}. The shift of the peak to a higher frequency is related to an increase in the N-acetylation extent and also the presence of hydrogen bonding.[33] In comparison to Bent−CS nanoclay, a shift to a lower frequency in the position band of the protonated amino group was observed. The peak appears at 1535 cm^{-1}, suggesting a strong electrostatic interaction with Bent as previously reported by other authors.[11,35] The band that appears at 1645 cm^{-1} in pure CS is related with the amide I band, and in Bent−CS nanoclay, the band that appears at 1633 cm^{-1} overlapped with the bending vibration band of water molecules adsorbed on Bent.[30]

The XRD assay was performed to find out if CS molecules were intercalated between Bent sheets as expected when a cationic exchange reaction takes place.[34] The parameter to monitor is the peak position, which shifts to lower angles as the interlamellar distance, d_{001}, increases.[32,36] Figure 2 shows the XRD patterns of Bent and Bent−CS powder registered at a low diffraction angle (2−10°).

The XRD pattern of Bent showed a reflection peak at $2\theta \sim 7.7°$, which corresponds to an interlamellar spacing of 11.5 Å (obtained using eq 1). After the incorporation of CS, the diffraction peak widens and shifts to approximately 5.6°, giving an interlamellar spacing of 15.6 Å. Thus, an increment of approximately 4 Å in Bent interlamellar distances was achieved. Similar results were obtained by several authors.[11,35,37] In agreement with these previous reports, CS molecules could be oriented in a monolayer arrangement between clay sheets, as depicted in Scheme 2.

TEM micrographs were taken to determine the shape, size, and interlamellar spacing of Bent and Bent−CS nanoclays. The micrographs, showed in Figure 3, confirmed that the silicate sheets of both nanoclays were arranged in tactoids, which consist

DOI: 10.1021/acs.jafc.8b00049
J. Agric. Food Chem. 2018, 66, 3101−3109

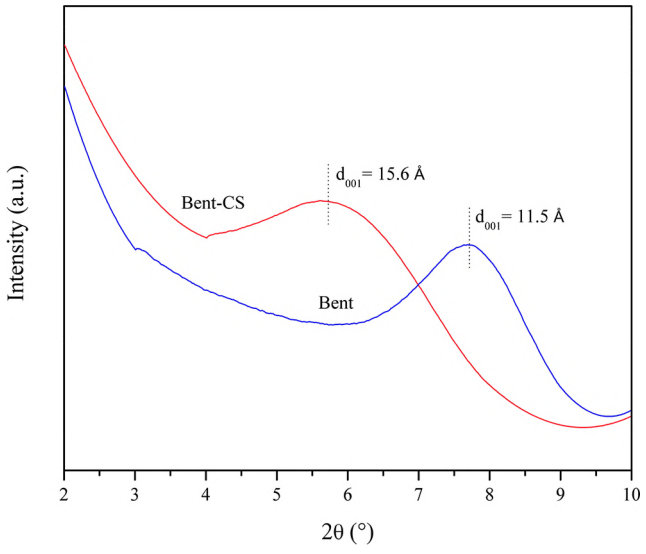

Figure 2. XRD patterns of Bent and Bent−CS nanoclay. CS intercalates between Bent sheets.

Scheme 2. Schematic Representation of CS Oriented in a Monolayer between Bent Sheets

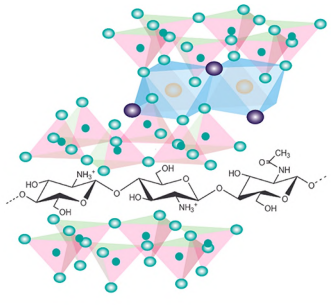

of the stacking of more than 10 sheets of about 1 nm thickness. Furthermore, the intercalation of the CS polymer between clay sheets was evident from the TEM micrograph analysis. The interlamellar spacing of Bent−CS nanoclay (16.04 Å) was found to be larger than that of Bent (11.32 Å), in which values are very close with those obtained by XRD.

The amount of CS supported in Bent−CS nanoclay was evaluated by TGA, and the curves are shown in Figure 4.

From the differential thermogravimetric analysis (DTGA) curves (Figure 4b), it can be seen that Bent degradation occurs mainly in two steps. The first step, between room temperature and 150 °C, is associated with desorption of water molecules (10.5%, w/w), and the other step, between 400 and 900 °C, is associated with the loss of a structural hydroxyl group (4.6%, w/w).[38] DTGA curves of CS show thermal degradation in three steps: room temperature−100, 200−350, and 350−572 °C, with mass losses of 5.9, 48, and 44%, respectively. Similar observations were reported by Liu et al.[39] The first mass loss is associated with water desorption; the second mass loss is associated with CS degradation and deacetylation; and the last mass loss is associated with the oxidative degradation of the carbonaceous residue produced in the previous step.[34] Bent−CS nanoclay also showed three degradation events. The first event, between room temperature and 156 °C, corresponds to the elimination of adsorbed water molecules, similar to that of Bent but with a comparatively inferior mass loss of 7.6% (w/w). The other two events appeared overlapped between 156 and 900 °C (13.6%, w/w), associated with CS degradation and Bent dehydroxylation.[39] The lower water loss in the first stage of Bent−CS TGA compared to that of Bent can be attributed to the formation of new interactions between Bent and CS, which produces a slight reduction of clay hydrophilicity.[24]

In addition, CS intercalated into Bent was determined using eqs 2 and 3. This way, it was found that Bent can host approximately 10% (w/w) of CS, and as observed by FTIR and XRD, its molecules would be oriented in a monolayer

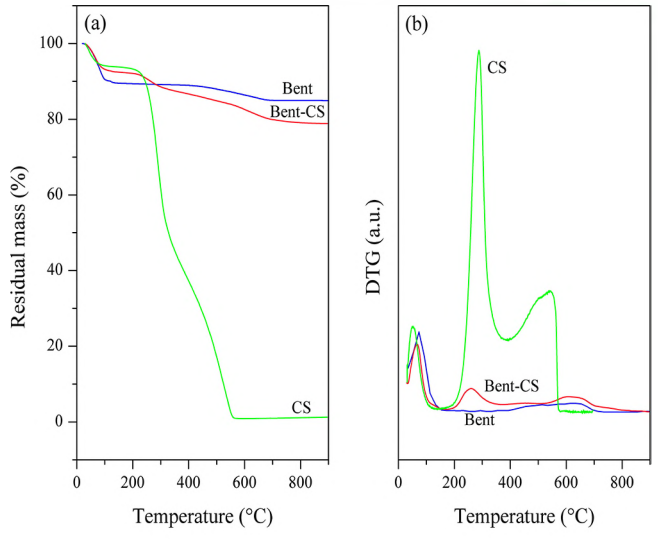

Figure 4. (a) TGA and (b) DTGA curves of Bent, Bent−CS, and CS.

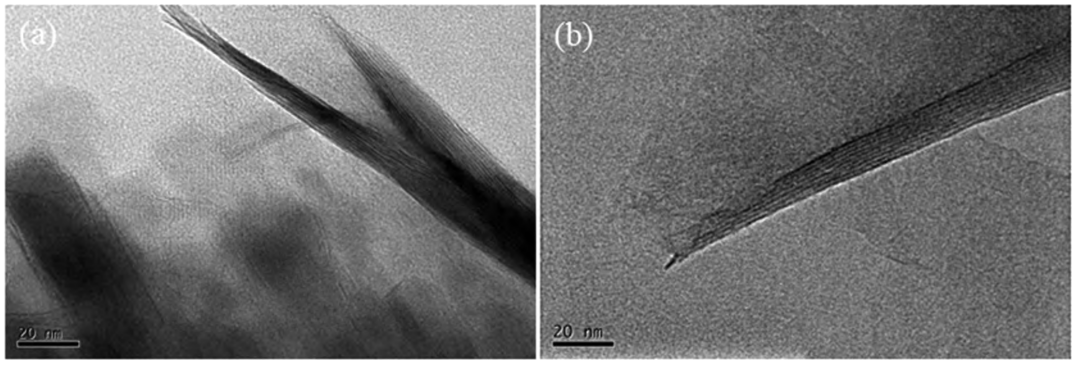

Figure 3. TEM images of (a) Bent and (b) Bent−CS nanoclays at 150000× magnification. Bar = 20 nm.

DOI: 10.1021/acs.jafc.8b00049
J. Agric. Food Chem. 2018, 66, 3101−3109

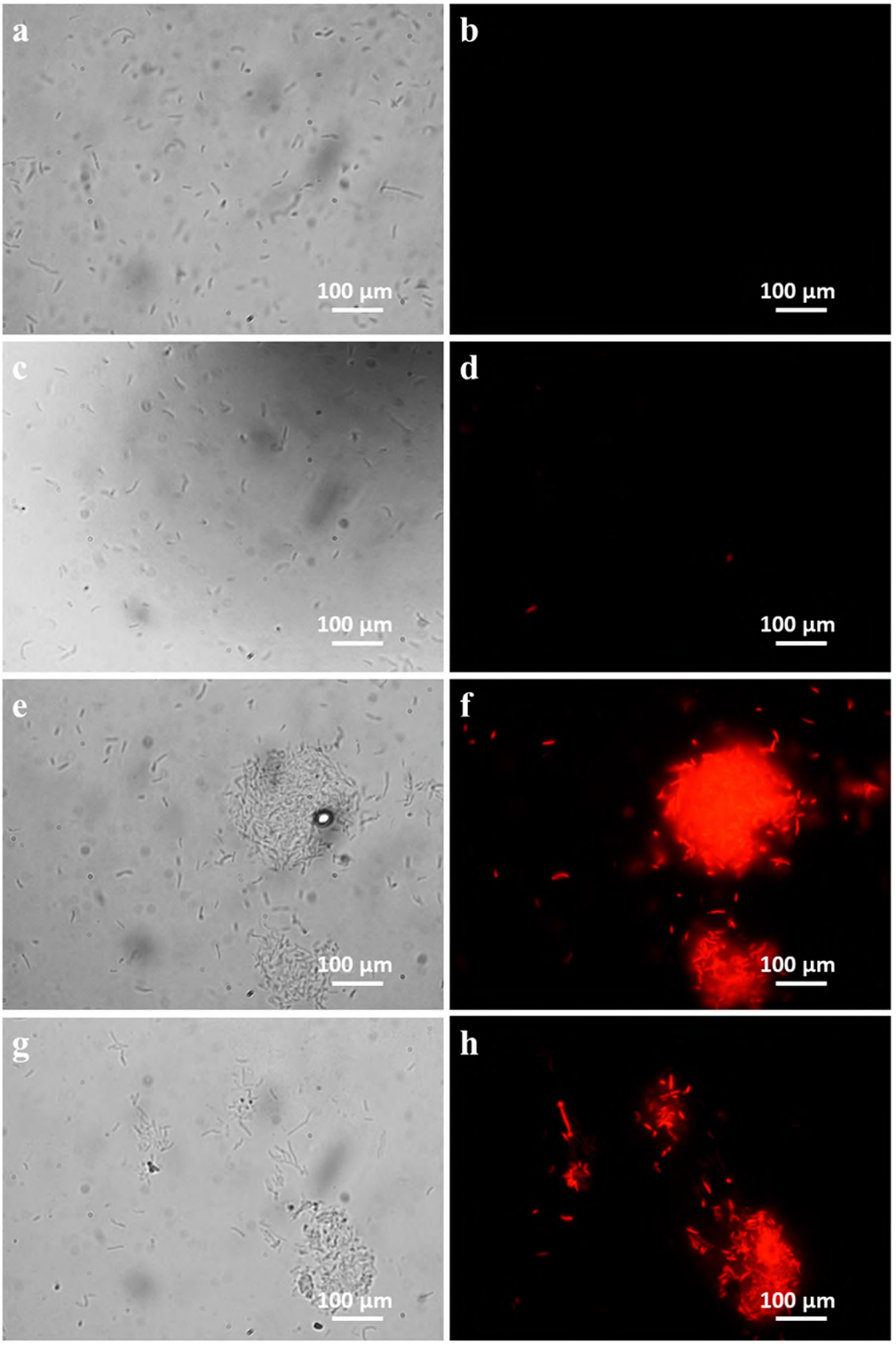

Figure 5. Bent−CS affects *Psy* cell viability. *Psy* cell suspensions were incubated with (a and b) 10 mg mL^{-1} Bent, (c and d) water, (e and f) 1 mg mL^{-1} CS (positive control), and (g and h) 10 mg mL^{-1} Bent−CS. Then, *Psy* cells were stained with PI dye and analyzed by (left panels) bright field microscope and (right panels) fluorescence microscope. Staining of *Psy* cells with PI resulted in an association of the dye with DNA, which still remains stable after lysis of the plasma membrane. Images are representative of three independent experiments. Bar = 100 μm.

arrangement between Bent sheets, interacting through electrostatic forces.

The antimicrobial activity of the Bent−CS nanoclays was investigated on the phytopathogens *Psy* and *F. eumartii* using PI to differentiate between living and dead cells. Clearly, Bent−CS exerted cell permeabilization in these two microorganisms, as revealed by the presence of PI-mediated fluorescence in nonviable cells (Figures 5 and 6). In comparison to controls (a, b, c, and d), a high level of fluorescence intensity was observed in *Psy* cells treated with Bent−CS (g and h) (Figure 5). As expected, CS used as a positive control had negative effects on bacteria cells (e and f). The antimicrobial activity of CS has been previously

DOI: 10.1021/acs.jafc.8b00049
J. Agric. Food Chem. 2018, 66, 3101−3109

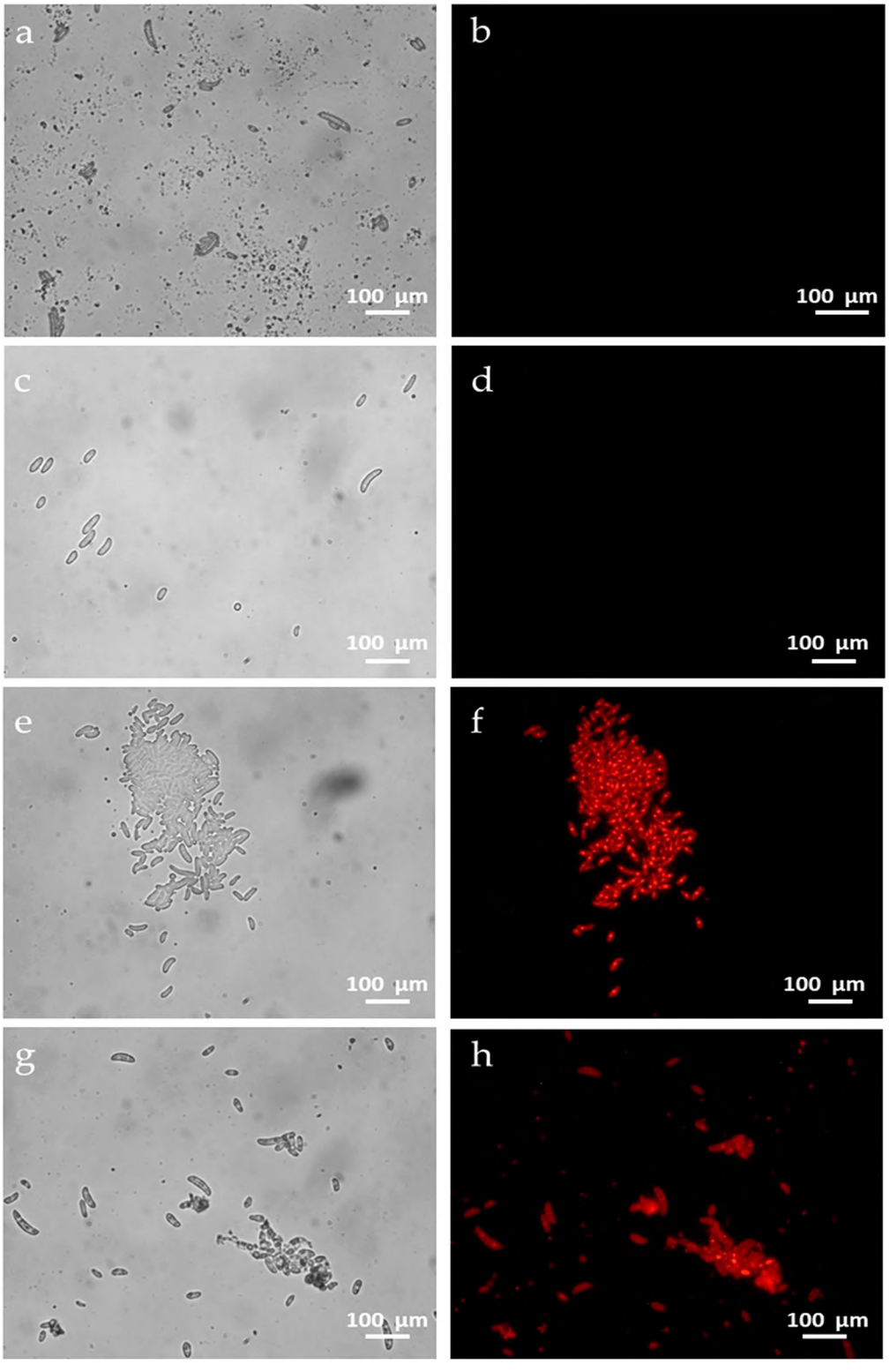

Figure 6. Bent−CS induces cell death in *F. eumartii* spores. Fungal spores were incubated with (a and b) water, (c and d) 10 mg mL^{-1} Bent, (e and f) 1 mg mL^{-1} CS (positive control), and (g and h) 10 mg mL^{-1} Bent−CS for 4 h. *F. eumartii* cells were stained with PI dye and analyzed by (left panels) bright field microscope and (right panels) fluorescence microscope. Images are representative of three independent experiments. Bar = 100 μm.

demonstrated in pathogenic bacteria, including *Xanthomonas*.[22,40]

Similar results were detected on the germination of *F. eumartii* spores (Figure 6). The antifungal properties have been also observed at different development stages, such as mycelial growth, sporulation, spore viability, and germination, and also on the production of fungal virulence factors.[41] Although fungi and bacteria can be inhibited, differential sensitivity to CS could be explained as a result of their different structures of cell walls.[42] Although different mechanisms have been proposed to explain the antimicrobial action of CS, none of them is mutually exclusive.[14]

DOI: 10.1021/acs.jafc.8b00049
J. Agric. Food Chem. 2018, 66, 3101−3109

Microorganisms are major crop pathogens. To protect themselves from biotic damage, plants have developed a wide variety of constitutive and inducible defenses, including pathogenesis-related proteins, such as chitinases and glucanases, proteinase inhibitors, reactive oxygen species (ROS), and expression of defense genes, among others.[44,45] The term elicitor is currently used for compounds stimulating any type of plant defense responses. Elicitors can be sprayed on crop plants to build up the natural defense system against microbial damage, such as could be the case of Bent−CS. CS could elicit plant defense response via electrostatic interactions with negatively charged phospholipids in the plant cell membranes.[46]. To evaluate the nanoclay Bent−CS elicitor properties, the levels of the glucanase protein PR2 accumulated in Bent and Bent−CS treated were analyzed by western blot (Figure 7). β-1,3-

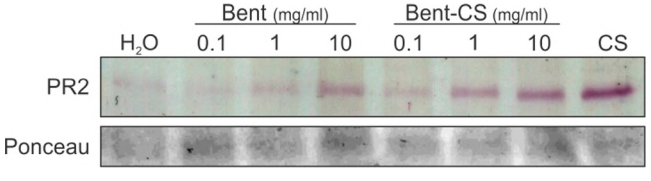

Figure 7. Western blot assay. Total protein extracts were obtained from 10-day-old tomato seedlings were sprayed with different concentrations of Bent or Bent−CS as shown. CS (0.1 mg/mL) was used as a positive control. After 24 h, total soluble proteins were extracted and analyzed by SDS−PAGE and transferred to a nitrocellulose membrane for immnodetection with the anti-PR2 glucanase antibody. Ponceau stain of the nitrocellulose membrane was used as the loading control.

Glucanase is one of the PR proteins (PR2). Previous reports revealed that CS was able to induce resistance by increasing β-1,3-glucanase activities in cucumbers, pears, and peaches.[43−45]

Clearly, the PR2 protein level was weakly detected in Bent but increased in a dose-dependent manner in Bent−CS-treated tomato plantlets. Again, as expected, CS as a control induced the PR2 level in tomato plantlets. Thus, our results revealed that, in addition to exerting antimicrobial effects, Bent−CS has associated elicitor activity, showing the preservation of CS activities. Previous studies showed that CS is not only an antimicrobial agent but also an effective elicitor of plant systemic acquired resistance to pathogens.[46] Because PR2 hydrolyzes glycans in the cell wall of many fungal and bacterial species, its role in plant defense responses has been previously speculated.[47,48]

CS antimicrobial and eliciting properties for pest control in plants have been very extensively studied.[46] Different cited reports demonstrate that CS exhibits inhibitory efficiency against bacteria, fungi, and viruses. These biological actions of CS have been explained by different mechanisms, including electrostatic interactions in the plasma membrane, CS−DNA/RNA interactions, among others.[49] In turn, CS has multiple applications associated with plant diseases by combining different properties and mechanisms.[50]

SEM micrographs of Bent and Bent−CS are presented in Figure 8. The visual analysis of Figure 8a allows for Bent an elucidation of a uniform and homogeneous appearance, with few irregularities. On the other hand, Figure 8b shows that Bent−CS has a more open or spongy structure with protuberances and irregularities. These visual results can be correlated with the increase in interlamellar spacing and the presence of parts of the CS chains outwardly or on the edges of the nanoclay, because a change in the Bent surface is clearly observed after its modification with CS. Similar results were reported by Ba et al.,[51] Ding et al.,[52] and Liu et al.[39] This observation together with the evidence found by FTIR and XRD could justify the antimicrobial action of Bent−CS observed on *Psy* and *F. eumartii* by offering this system direct contact between CS and these pathogens.

This way, novel sustainable nanoclay for agricultural application has been obtained by combining Bent-hosting capacity with the cationic polysaccharide, CS. Results from FTIR, TGA, and XRD indicated that CS interacts with Bent through strong electrostatic interactions and intercalates Bent sheets mostly in a monolayer arrangement. The amount of CS stored in Bent−CS was 10% (w/w). The assayed antimicrobial activity against bacterial and fungal phytopathogens showed that the effectiveness of CS was preserved in Bent−CS nanoclays. Then, facing current agriculture, the application of Bent−CS by foliar spray could be an ecofriendly and non-hazardous tool to control phytopathogens in tomato crops.

■ ASSOCIATED CONTENT

Supporting Information

The Supporting Information is available free of charge on the ACS Publications website at DOI: 10.1021/acs.jafc.8b00049.

Performance of CS intercalation in Bent (Figure S1) (PDF)

■ AUTHOR INFORMATION

Corresponding Author

*Telephone: +54-223-626-0600. E-mail: danila.merino@fi.mdp.edu.ar.

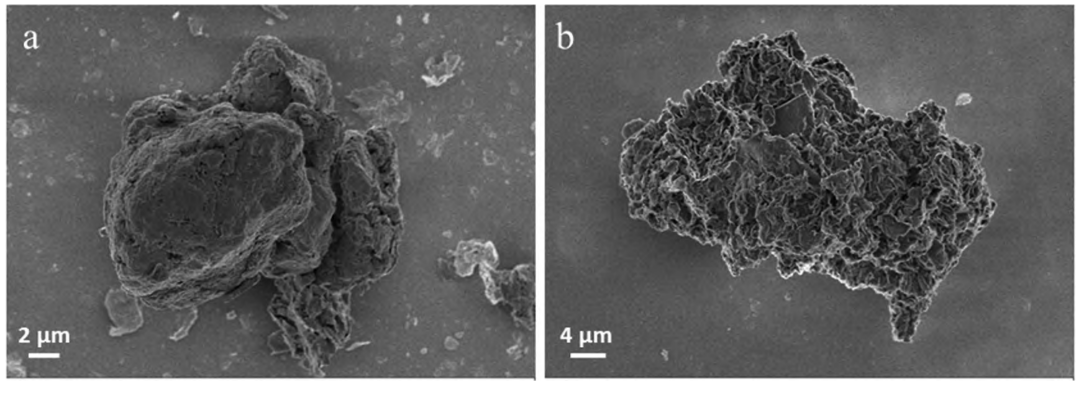

Figure 8. SEM micrographs of (a) Bent and (b) Bent−CS.

DOI: 10.1021/acs.jafc.8b00049
J. Agric. Food Chem. 2018, 66, 3101−3109

ORCID

Danila Merino: 0000-0002-5098-8550

Funding

The authors acknowledge the financial support of the National Research Council (CONICET), the National Agency for Scientific and Technical Promotion (ANPCyT) and the National University of Mar del Plata (UNMdP).

Notes

The authors declare no competing financial interest.

■ ACKNOWLEDGMENTS

The authors thank Dr. Vanesa Muñoz for the amazing TEM images that she took, Dr. Tomy Gutierrez for the acquired SEM images, and ID Ezequiel Macri for the "table of contents" realization.

■ ABBREVIATIONS USED

Bent, bentonite; CS, chitosan; *Psy*, *Pseudomonas syringae* pv. *tomato* DC3000; *F. eumartii*, *Fusarium solani* f. sp. *eumartii*; FTIR, Fourier transform infrared spectroscopy; XRD, X-ray diffraction; TGA, thermogravimetric analysis; SEM, scanning electron microscopy; TEM, transmission electron microscopy

■ REFERENCES

(1) Chen, H.; Yada, R. Nanotechnologies in agriculture: New tools for sustainable development. *Trends Food Sci. Technol.* **2011**, *22* (11), 585−594.

(2) Anderson, J. A.; Gipmans, M.; Hurst, S.; Layton, R.; Nehra, N.; Pickett, J.; Shah, D. M.; Souza, T. L. P. O.; Tripathi, L. Emerging agricultural biotechnologies for sustainable agriculture and food security. *J. Agric. Food Chem.* **2016**, *64* (2), 383−393.

(3) Nazir, M. S.; Mohamad Kassim, M. H.; Mohapatra, L.; Gilani, M. A.; Raza, M. R.; Majeed, K. Characteristic properties of nanoclays and characterization of nanoparticulates and nanocomposites. In *Nanoclay Reinforced Polymer Composites*; Jawaid, M., Qaiss, A. K., Bouhfid, R., Eds.; Springer: Singapore, 2016; pp 35−55, DOI: 10.1007/978-981-10-1953-1_2.

(4) Uddin, F. Clays, nanoclays, and montmorillonite minerals. *Metall. Mater. Trans. A* **2008**, *39* (12), 2804−2814.

(5) Czaban, J.; Siebielec, G. Effects of bentonite on sandy soil chemistry in a long-term plot experiment (II); effect on pH, CEC, and macro- and micronutrients. *Pol. J. Environ. Stud.* **2013**, *22* (6), 1669−1676.

(6) Satje, A.; Nelson, P. Bentonite treatments can improve the nutrient and water holding capacity of sugarcane soils in the wet tropics. *Proc. Aust. Soc. Sugar Cane Technol.* **2009**, *31*, 166−176.

(7) Mi, J.; Gregorich, E. G.; Xu, S.; McLaughlin, N. B.; Ma, B.; Liu, J. Effect of bentonite amendment on soil hydraulic parameters and millet crop performance in a semi-arid region. *F. Crop. Res.* **2017**, *212*, 107−114.

(8) Qadir, M.; Noble, A. D.; Chartres, C. Adapting to climate change by improving water productivity of soils in dry areas. *L. Degrad. Dev.* **2013**, *24* (1), 12−21.

(9) Semalulu, O.; Elobu, P.; Namazzi, S.; Kyebogola, S.; Mubiru, D. N. Higher cereal and legume yields using Ca-bentonite on sandy soils in the dry eastern uganda: Increased productivity versus profitability. *Univers. J. Agric. Res.* **2017**, *5* (2), 140−147.

(10) Codex Alimentarius Commission (CAC). *Organically Produced Foods*, 3rd ed.; CAC: Rome, Italy, 2007.

(11) Monvisade, P.; Siriphannon, P. Chitosan intercalated montmorillonite: Preparation, characterization and cationic dye adsorption. *Appl. Clay Sci.* **2009**, *42* (3), 427−431.

(12) Zubareva, A. A.; Ilyina, A. V.; Levov, A. N.; Zueva, V. S.; Svirshchevskaya, E. V.; Varlamov, V. P. Protein delivery by nanoparticles formed by chitosan-*N*-acyl derivatives. *Prog. Chem. Appl. Chitin Its Deriv.* **2011**, *XVI*, 61−70.

(13) Wang, X.; Chi, N.; Tang, X. Preparation of estradiol chitosan nanoparticles for improving nasal absorption and brain targeting. *Eur. J. Pharm. Biopharm.* **2008**, *70* (3), 735−740.

(14) Orzali, L.; Corsi, B.; Forni, C.; Riccioni, L. Chitosan in agriculture: A new challenge for managing plant disease. In *Biological Activities and Application of Marine Polysaccharides*; Shalaby, E. A., Ed.; InTech: Rijeka, Croatia, 2017; Chapter 2, DOI: 10.5772/66840.

(15) Malerba, M.; Cerana, R. Chitosan effects on plant systems. *Int. J. Mol. Sci.* **2016**, *17* (7), 996.

(16) Zhang, X.; Li, K.; Liu, S.; Zou, P.; Xing, R.; Yu, H.; Chen, X.; Qin, Y.; Li, P. Relationship between the degree of polymerization of chitooligomers and their activity affecting the growth of wheat seedlings under salt stress. *J. Agric. Food Chem.* **2017**, *65* (2), 501−509.

(17) Ravi Kumar, M. N. A review of chitin and chitosan applications. *React. Funct. Polym.* **2000**, *46* (1), 1−27.

(18) Chittenden, C.; Singh, T. In vitro evaluation of combination of *Trichoderma harzianum* and chitosan for the control of Sapstain fungi. *Biol. Control* **2009**, *50* (3), 262−266.

(19) López-Mondéjar, R.; Blaya, J.; Obiol, M.; Ros, M.; Pascual, J. A. Evaluation of the effect of chitin-rich residues on the chitinolytic activity of *Trichoderma harzianum*: In vitro and greenhouse nursery experiments. *Pestic. Biochem. Physiol.* **2012**, *103* (1), 1−8.

(20) Khalil, M. S.; Badawy, M. E. I. Nematicidal activity of a biopolymer chitosan at different molecular weights against root-knot nematode, *Meloidogyne incognita*. *Plant Prot. Sci.* **2012**, *48* (4), 170−178.

(21) Antón, A.; Torrellas, M.; Núñez, M.; Sevigné, E.; Amores, M. J.; Muñoz, P.; Montero, J. I. Improvement of agricultural life cycle assessment studies through spatial differentiation and new impact categories: Case study on greenhouse tomato production. *Environ. Sci. Technol.* **2014**, *48* (16), 9454−9462.

(22) Mansilla, A. Y.; Albertengo, L.; Rodríguez, M. S.; Debbaudt, A.; Zúñiga, A.; Casalongué, C. A. Evidence on antimicrobial properties and mode of action of a chitosan obtained from crustacean exoskeletons on *Pseudomonas syringae* pv. *tomato* DC3000. *Appl. Microbiol. Biotechnol.* **2013**, *97* (15), 6957−6966.

(23) Terrile, M. C.; Mansilla, A. Y.; Albertengo, L.; Rodríguez, M. S.; Casalongué, C. A. Nitric-oxide-mediated cell death is triggered by chitosan in *Fusarium eumartii* spores. *Pest Manage. Sci.* **2015**, *71* (5), 668−674.

(24) Merino, D.; Ollier, R.; Lanfranconi, M.; Alvarez, V. Preparation and characterization of soy lecithin-modified bentonites. *Appl. Clay Sci.* **2016**, *127*−*128*, 17−22.

(25) Murashige, T.; Skoog, F. A revised medium for rapid growth and bio assays with tobacco tissue cultures. *Physiol. Plant.* **1962**, *15* (3), 473−497.

(26) King, E. O.; Ward, M. K.; Raney, D. E. Two simple media for the demonstration of pyocyanin and fluorescin. *J. Lab. Clin. Med.* **1954**, *44* (2), 301−307.

(27) Novo, D. J.; Perlmutter, N. G.; Hunt, R. H.; Shapiro, H. M. Multiparameter flow cytometric analysis of antibiotic effects on membrane potential, membrane permeability, and bacterial counts of *Staphylococcus aureus* and *Micrococcus luteus*. *Antimicrob. Agents Chemother.* **2000**, *44* (4), 827−834.

(28) Arndt-Jovin, D. J.; Jovin, T. M. Fluorescence labeling and microscopy of DNA. *Methods Cell Biol.* **1989**, *30*, 417−448.

(29) Laemmli, U. K. Cleavage of structural proteins during the assembly of the head of bacteriophage T4. *Nature* **1970**, *227* (5259), 680−685.

(30) Darder, M.; Colilla, M.; Ruiz-Hitzky, E. Biopolymer-clay nanocomposites based on chitosan intercalated in montmorillonite. *Chem. Mater.* **2003**, *15* (20), 3774−3780.

(31) Nayak, P. S.; Singh, B. K. Instrumental characterization of clay by XRF, XRD and FTIR. *Bull. Mater. Sci.* **2007**, *30* (3), 235−238.

(32) Günister, E.; Pestreli, D.; Ünlü, C. H.; Atıcı, O.; Güngör, N. Synthesis and characterization of chitosan-MMT biocomposite systems. *Carbohydr. Polym.* **2007**, *67* (3), 358−365.

(33) Domszy, J. G.; Roberts, G. A. F. Evaluation of infrared spectroscopic techniques for analysing chitosan. *Makromol. Chem.* **1985**, *186* (8), 1671−1677.

DOI: 10.1021/acs.jafc.8b00049
J. Agric. Food Chem. 2018, 66, 3101−3109

(34) Wang, S. F.; Shen, L.; Tong, Y. J.; Chen, L.; Phang, I. Y.; Lim, P. Q.; Liu, T. X. Biopolymer chitosan/montmorillonite nanocomposites: Preparation and characterization. *Polym. Degrad. Stab.* **2005**, *90* (1), 123−131.
(35) Han, Y.-S.; Lee, S.-H.; Choi, K. H.; Park, I. Preparation and characterization of chitosan−clay nanocomposites with antimicrobial activity. *J. Phys. Chem. Solids* **2010**, *71* (4), 464−467.
(36) Rhim, J.-W.; Hong, S.-I.; Park, H.-M.; Ng, P. K. W. Preparation and characterization of chitosan-based nanocomposite films with antimicrobial activity. *J. Agric. Food Chem.* **2006**, *54* (16), 5814−5822.
(37) Darder, M.; Colilla, M.; Ruiz-Hitzky, E. Chitosan−clay nanocomposites: Application as electrochemical sensors. *Appl. Clay Sci.* **2005**, *28* (1), 199−208.
(38) Futalan, C. M.; Kan, C.-C.; Dalida, M. L.; Hsien, K.-J.; Pascua, C.; Wan, M.-W. Comparative and competitive adsorption of copper, lead, and nickel using chitosan immobilized on bentonite. *Carbohydr. Polym.* **2011**, *83* (2), 528−536.
(39) Liu, Q.; Yang, B.; Zhang, L.; Huang, R. Adsorption of an anionic azo dye by cross-linked chitosan/bentonite composite. *Int. J. Biol. Macromol.* **2015**, *72*, 1129−1135.
(40) Li, B.; Wang, X.; Chen, R.; Huangfu, W.; Xie, G. Antibacterial activity of chitosan solution against Xanthomonas pathogenic bacteria isolated from Euphorbia pulcherrima. *Carbohydr. Polym.* **2008**, *72* (2), 287−292.
(41) Badawy, M. E. I.; Rabea, E. I. A biopolymer chitosan and its derivatives as promising antimicrobial agents against plant pathogens and their applications in crop protection. *Int. J. Carbohydr. Chem.* **2011**, *2011*, 1−29.
(42) Xing, K.; Zhu, X.; Peng, X.; Qin, S. Chitosan antimicrobial and eliciting properties for pest control in agriculture: A review. *Agron. Sustainable Dev.* **2015**, *35* (2), 569−588.
(43) El Ghaouth, A.; Arul, J.; Grenier, J.; Benhamou, N.; Asselin, A.; Bélanger, R. Effect of chitosan on cucumber plants: Suppression of *Pythium aphanidermatum* and induction of defense reactions. *Phytopathology* **1994**, *84* (3), 313−320.
(44) Ma, Z.; Yang, L.; Yan, H.; Kennedy, J. F.; Meng, X. Chitosan and oligochitosan enhance the resistance of peach fruit to brown rot. *Carbohydr. Polym.* **2013**, *94* (1), 272−277.
(45) Meng, X.; Yang, L.; Kennedy, J. F.; Tian, S. Effects of chitosan and oligochitosan on growth of two fungal pathogens and physiological properties in pear fruit. *Carbohydr. Polym.* **2010**, *81* (1), 70−75.
(46) Xing, K.; Zhu, X.; Peng, X.; Qin, S. Chitosan antimicrobial and eliciting properties for pest control in agriculture: A review. *Agron. Sustainable Dev.* **2015**, *35* (2), 569−588.
(47) van Loon, L. C.; Rep, M.; Pieterse, C. M. J. Significance of inducible defense-related proteins in infected plants. *Annu. Rev. Phytopathol.* **2006**, *44* (1), 135−162.
(48) Wróbel-Kwiatkowska, M.; Lorenc-Kukula, K.; Starzycki, M.; Oszmiański, J.; Kepczyńska, E.; Szopa, J. Expression of β-1,3-glucanase in flax causes increased resistance to fungi. *Physiol. Mol. Plant Pathol.* **2004**, *65* (5), 245−256.
(49) Rabea, E. I.; Badawy, M. E. T.; Stevens, C. V.; Smagghe, G.; Steurbaut, W. Chitosan as antimicrobial agent: applications and mode of action. *Biomacromolecules* **2003**, *4* (6), 1457−1465.
(50) Hadwiger, L. A. Multiple effects of chitosan on plant systems: Solid science or hype. *Plant Sci.* **2013**, *208*, 42−49.
(51) Ba, K.; He, L. L.; Tang, H.; Gao, J. Q.; Zhu, S. F.; Li, Y.; Sun, W. N. Use of chitosan-modified bentonite for removal of Cu^{2+}, Cl^{-} and 2,4-dichlorophenoxyacetic acid (2,4-D) from aqueous solution. *Kem. Ind.* **2014**, *63* (7−8), 253−258.
(52) Ding, C.; Gong, D.; Yu, P.; Shao, J.; Zhong, M.-E. Removal of quinclorac herbicide from aqueous solution by chitosan/montmorillonite bionanocomposite. *Desalin. Water Treat.* **2016**, *57* (52), 24970−24981.

DOI: 10.1021/acs.jafc.8b00049
J. Agric. Food Chem. 2018, 66, 3101−3109